

Original Article

Evaluation of Misclassification Matrix Method in Validation of an Assistive Device for Manual Wheelchair Propulsion

M. H. Muhammad Sidik¹, S. A. Che Ghani², Abdul Nasir³, M.N.F. Saniman⁴

^{1,2}Mechanical and Automotive Engineering Technology, Universiti Malaysia Pahang, Pahang, Malaysia

³Electrical and Electronics Engineering Technology, Universiti Malaysia Pahang, Pahang, Malaysia

⁴Department of Mechanical Engineering, Universiti Kuala Lumpur, Bangi, Selangor, Malaysia

¹Corresponding Author : mohdhanafi88@gmail.com

Received: 15 July 2022

Revised: 31 October 2022

Accepted: 30 November 2022

Published: 24 December 2022

Abstract - Classification accuracy is essential in the bio signal's performance-based assistive devices. In this study, surface electromyography (SEMG) signals acquisition was extracted from 3 healthy right-handed participants. SEMG signal was processed, and Motor Unit Action Potential (MUAP) was determined. Accuracy, precision, sensitivity and specificity were calculated in real-time based on individual MUAP, critically compared with pattern and non-pattern recognition control methods by Misclassification Matrix inserted into Arduino MEGA 2560 Microcontroller. The results indicated that the performance of each control method is different for every participant and a comparison tool is a must to select the best out of it. It shows that the misclassification matrix filtered the best control method for participant 1 as Probability Density Function, no for participant 2 and Maximum Point Different (MPD) for participant 3 based on determined conditions.

Keywords - Arduino, Misclassification matrix, MUAP, Surface electromyography, Wheelchair propulsion.

1. Introduction

Muscle-generated currents during a contraction to indicate neuro-muscular activities are called Surface Electromyography (SEMG) signal¹. Condition of muscles either in relaxing or contraction is generating SEMG signal and being monitored by the nervous system^{2,3}. It depends on the muscle's characteristics, physiological and anatomical. Noise can occur while the SEMG signal is conducted through tissues⁴. Meanwhile, the signal generated during the contraction of the cell is known as action potential activated by electrical current.

Physiological changes in muscle fibre membrane will generate the myoelectric signal⁵⁻⁷. This myoelectrical signal is represented as an EMG signal. Then, the EMG is acquired on the skin surface and recognised as SEMG signal^{8,9}. SEMG signals a function of time and can be represented in the form of amplitude, phase and frequency.

SEMG signal is measurable using the bio-medical technique that focuses on changes, recording, investigating and assessing the myoelectrical signal¹⁰. Many SEMG data acquisition devices are available on the market being used for research and clinical applications^{11,12}

SEMG signal is one of the bio-signals used in most rehabilitation assistive robots, such as exoskeletons. Control strategies for the devices can be classified into two, which are pattern and non-pattern recognition control methods. Non-pattern recognition is much simpler compared to pattern recognition by implementing the ON/OFF type of controller by referring to the threshold value. Meanwhile, the pattern recognition-based approach for SEMG signal has 4 steps (acquisition, segmentation, extraction and classification) before any judgment is made, as in Figure 1.

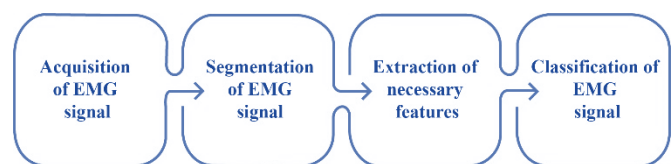


Fig. 1 Steps for pattern recognition-based approach

Due to more complex decision-making steps, the pattern recognition control method is more accurate than the non-pattern one¹³. Classification accuracy will be the end result to be used as the main factor in choosing which control method suits each participant the most. Classification accuracy for most of the studies on SEMG conducted is not obtained in real-time. The accuracy is measured after the



experiment ends. Meanwhile, classification accuracy is measured and calculated in real-time for this study.

2. Materials and Methods

2.1. Experimental Design

Placement on the muscle's location is referred to by the Non-Invasive Assessment of Muscles (SENIAM) guideline, and the reference electrodes were placed on an electrically neutral muscle close to the targeted muscle. sEMG sensor 1 is on BIC; meanwhile, sEMG sensor 2 is on TRI, as in Figure 2. The brachialis is the muscle for reference electrodes sensors 1 and 2

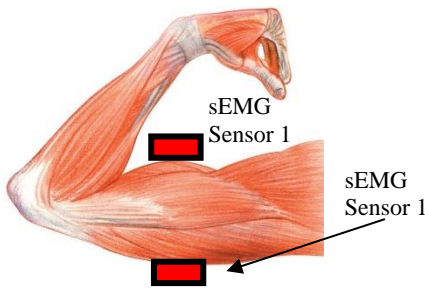


Fig. 2 Placement of sEMG sensors on Biceps Brachii and Triceps Brachii muscles

The experiment process consists of 5 contact and 5 recovery phases, as in Figure 4. Participants have to perform only one activity and repeat 5 times in each contact and recovery phase based on the time period.

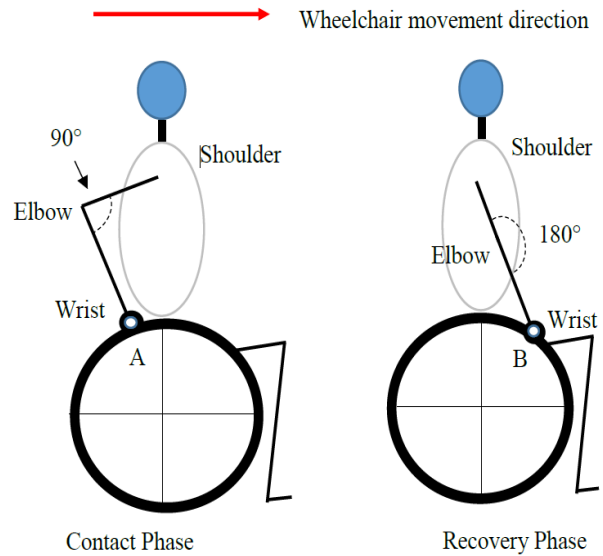


Fig. 3 Hand movement and position in contact and recovery phase

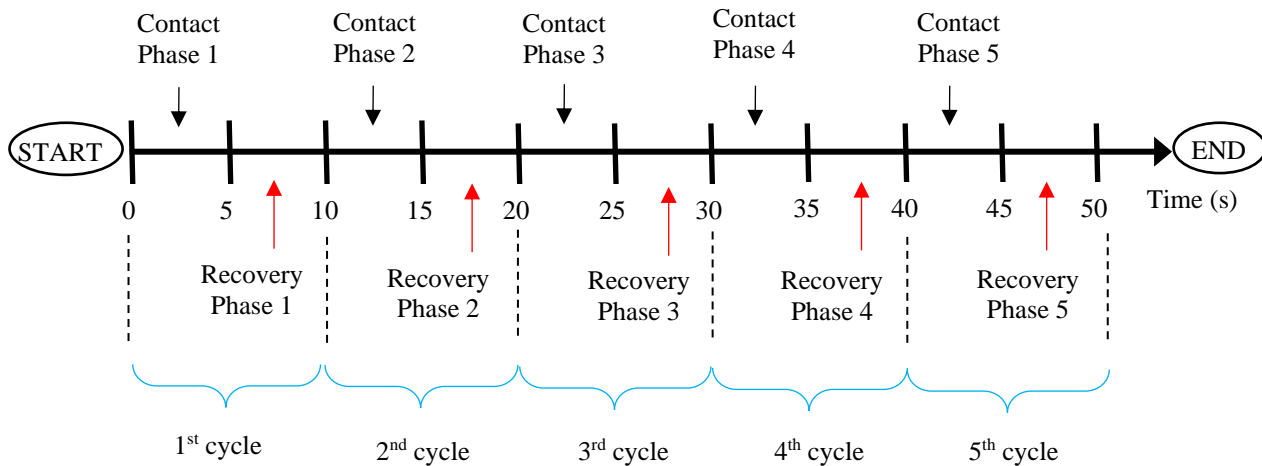


Fig. 4 Experiment timeline

There are two phases of propelling a manual wheelchair, contact and recovery. Figure 3 illustrates the hand position in both phases. The contact phase starts from point A to point B and the recovery phase from point B to A. Origin position A depends on each participant's arm's length, and to standardize it, the shoulder-elbow-wrist angle must be at 90° , and this position is determined before the experiment starts to maximize the force transferred from arm to wheelchair pushrim, and the angle of shoulder-elbow-wrist had to be at 90° ¹⁴.

0s – 5s is contact phase, 5s – 10s is recovery phase, 10s – 15s is contact phase, 15s – 20s is recovery phase, 20s – 25s is contact phase, 25s – 30s is recovery phase, 30s – 35s is contact phase, 35s – 40s is recovery phase, 40s – 45s is contact phase and 45s – 50s is recovery phase. 1 cycle consists of 1 contact and 1 recovery phase. For the whole experiment has 5 cycles of hand movement.

3 healthy humans participated in the SEMG data collection experiment using Myoware Muscle Sensor (SEM-13723) and Arduino MEGA 2560 Microcontroller. Their

details are as in Table 1. Institutional Review Board¹³ approved the experiments and briefed the participants before they signed the consent form. Prior to the experiment, a training session for the subject to get used to wheelchair propulsion was given for 12 minutes¹⁶⁻¹⁸. Participants' handedness is not considered in this experiment.

2.2. SEMG Classification

Classification techniques are identified based on participants' hand movements sensed by SEMG sensors. Then, these EMG signals were used to feed the information to classifiers to determine which phases participants were currently on. Classification accuracy depends much on the sampling rate. The higher, the better. However, there is a limitation for the Arduino MEGA 2560 microcontroller, which has a sampling rate of up to 407 Hz.

Based on studies, the difference in classification accuracy among sampling rates 1000Hz and 400Hz is just around 0.43%. Therefore, 400Hz can be a minimum level of sampling rate for sEMG data acquisition device¹⁹⁻²¹. This study implemented two types of classifiers: pattern and non-pattern recognition control methods. Both control methods were tested in real-time and compared using a misclassification matrix regarding classification accuracy.

2.3. Misclassification Matrix

The evaluation of SEMG signal classification accuracy methods can be obtained in terms of correctness by statistical computing calculations called the True Negatives (TN), True Positives (TP), False Negatives (FN) and False Positives (FP). Component form of misclassification matrix as in Figure 5. A classification Matrix is a table developed for classifiers on a binary data set, used to validate and compare the performance of each classifier.

In the classification matrix, observations classified correctly into the positive class are known as True Positives (TP), and True Negatives (TN) are the negative class. Instances of the positive class classified falsely as negative are called False Negatives (FN), and instances of the negative class classified falsely as positive are called FP²³. Classifiers' performance can be calculated based on frequencies in each class by determining the classification accuracy. Furthermore, precision = TP / (TP+FP), sensitivity = TP / (TP+FN), specificity = TN / (TN+FP) and accuracy = (TP+TN) / (TP+TN+FP+FN) can be determined too.

Table 1. Details of Participant

Participant	1	2	3
Gender	Male	Male	Male
Age (Year)	20	24	24
Height (cm)	156	159	171
Weight (kg)	49	49	56
Average Contact Time (s)	1.63	1.71	2.12
Average Recovery Time (s)	1.76	1.35	1.33

	Predicted: No	Predicted: Yes
Actual: No	TN	FP
Actual: Yes	FN	TP

Fig. 5 Misclassification matrix classes

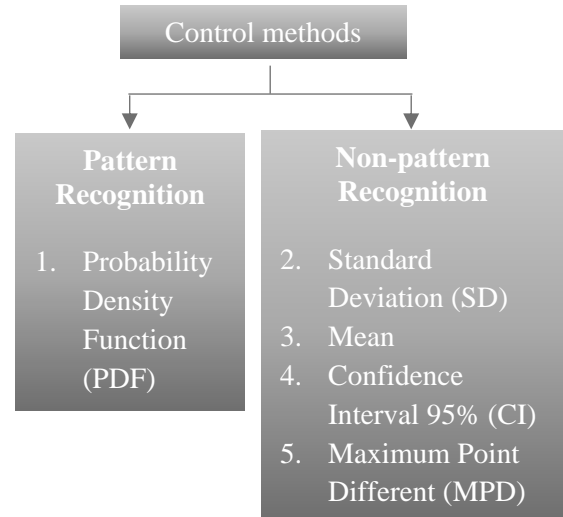


Fig. 6 Control methods

In this paper, a confusion matrix is used as a tool for the algorithm to select the most suitable control method (classifiers) to be chosen for assistive manual wheelchair propulsion. 3 participants were volunteered to participate in this study to find the best control method that suited them. 2 types of control methods that are installed in the control units which are pattern recognition (Probability Density Function (PDF)) and non-pattern recognition (confidence interval (CI), Standard Deviation (SD), mean and maximum point different (MPD)) as in Figure 6.

The mean and standard deviation (SD) for every participant was determined using Equations 1 and 2. x is the maximum MUAP for each contact and recovery phase, N is the total number of phases which is 5, \bar{x} is the mean, and σ is SD.

$$\bar{x} = \frac{\sum x}{N} \tag{1}$$

$$\sigma = \sqrt{\frac{1}{N} \sum (x - \bar{x})^2} \tag{2}$$

Confidence interval (CI) is a range of values that is possibly 95% certain and contains the population's true mean. 95% and 99% are the common CIs, but most researchers use 95% for EMG applications to analyze data²⁴. CI calculated using Equation 3, N is the total number of phases which is 5, \bar{x} is the mean, and σ is the SD value of MUAP.

Table 2. Rubrics for control method assessment

Control method	“1”	“0”
Non-Pattern recognition	MUAP surpass threshold	MUAP below threshold
Pattern recognition	The probability is higher for the contact phase pattern	The probability is higher for the recovery phase pattern

$$CI = \bar{x} \pm 1.960 \frac{\sigma}{\sqrt{N}} \quad (3)$$

MPD was introduced to find the difference in terms of voltage for contact and recovery phase as in Equation 4. That different point will be an indicator for determining the threshold for method selection. All maximum points in contact and recovery phases will be checked either over or equal to 0.5V to 5.0V for the increment of 0.1V.

$$MPD (V) = Max Contact - Max recovery \quad (4)$$

Equation PDF as in Equation 5. PDF comparing probability between two values from the contact phase and recovery phase to discern which one has the higher value. If the probability is higher for the value in contact, command “1” will be sent to the power-assist system to switch on. Meanwhile, the signal remains “0” when the probability of recovery is higher.

$$F(x) = \frac{1}{\sqrt{2\pi}\sigma} e^{-\frac{(x-\mu)^2}{2\sigma^2}} \quad (5)$$

- e = 2.71828
- π = 3.14159
- μ = Means
- σ = Standard deviation
- X = sEMG value

Evaluation of how the point is given to each control method is as in Table 2. Positive is when MUAP is over than threshold, and negative is below the threshold for non-pattern recognition. Meanwhile, in pattern recognition, the probability higher for the pattern in the contact phase is positive and negative for the recovery phase. For the contact phase, the focus will be on TP to determine when MUAP exceeds thresholds, and 1 point is given when it happens.

The identical method was applied in the recovery phase, 1 point for every time MUAP surpassed the threshold values for each method and placed under FN. The total points in both phases are calculated by Arduino Mega 2560 microcontroller to sort out the best methods.

2.4. Assessment on Control Methods

The misclassification matrix offers a powerful way to establish how reliable the measurement of a MUAP is and

how well-defined the selection methods in the classification scheme are. The misclassification matrix is an assessment method to sort out which is the best method that suits each participant. True Positives (TP) and false Negatives (FN) are essential to look into, and some conditions are implemented for filtering the best control method. In the misclassification matrix, TP will be used in the contact phase, and FN is in the recovery phase. TP is when signal “1” is produced at the right time, and FN when signal “1” was produced at the wrong time.

SEMG signals are extracted from BIC and TRI muscles. Results separated for each phase and total count of “0” and “1” were calculated to find the value of TP and FN, as shown in Figure 7. For BIC, TRI group. The total counts of “0” and “1” are different in every phase due to the speed of the laptop’s processor to display the data. “0” shows that MUAP from both muscle groups did not go over than threshold value.

“1” indicates both muscle groups MUAP are bigger than thresholds at the same time. Looking at the PDF using individual data for BIC and TRI, in the 1st and 5th cycle there is none “1” appeared. But in the 2nd cycle (9 times in the contact phase), 3rd cycle (1 time in contact phase) and 4th cycle (7 times in contact phase).

3. Results

Figure 8 is the SEMG signal obtained from one of the participants. From the observation on the graph, there are differences in maximum MUAP value for contact, which are higher compared to the recovery phase in every cycle. Every time an activity was performed in each phase, the MUAP value suddenly rose and fell just after. This is where muscles contracted during forward stroke, hand return, and MUAP remain low when the participant is relaxed and waiting for another phase.

Table 3 and 4 shows threshold values for non-pattern and pattern recognition control method obtained from individual MUAP implemented into Arduino MEGA 2560 and will be assessed using a misclassification matrix later. NA in Table 3 means that there is no MUAP in the contact phase with a higher voltage than in the recovery phase.

Table 3. Non-pattern recognition control method threshold

Participant	Muscle Group	Mean (V)	SD (V)	CI (V)	MPD (V)
1	BIC	1.52	1.84	1.80	NA
	TRI	1.95	3.55	3.35	NA
2	BIC	3.45	3.57	3.56	NA
	TRI	1.42	2.03	1.95	NA
3	BIC	3.74	3.86	3.84	3.5
	TRI	2.78	2.94	2.92	2.6

Table 4. Mean and SD value used for PDF

Participant	Muscle group		Contact		Recovery	
			Mean (V)	SD (V)	Mean (V)	SD (V)
1	BIC		1.52	0.32	1.36	0.44
	TRI		1.95	1.60	3.71	1.59
2	BIC	3.45	0.12	3.37		0.15
	TRI	1.42	0.60	2.24		1.41
3	BIC	3.74	0.12	2.24		0.86
	TRI	2.78	0.15	2.52		1.29

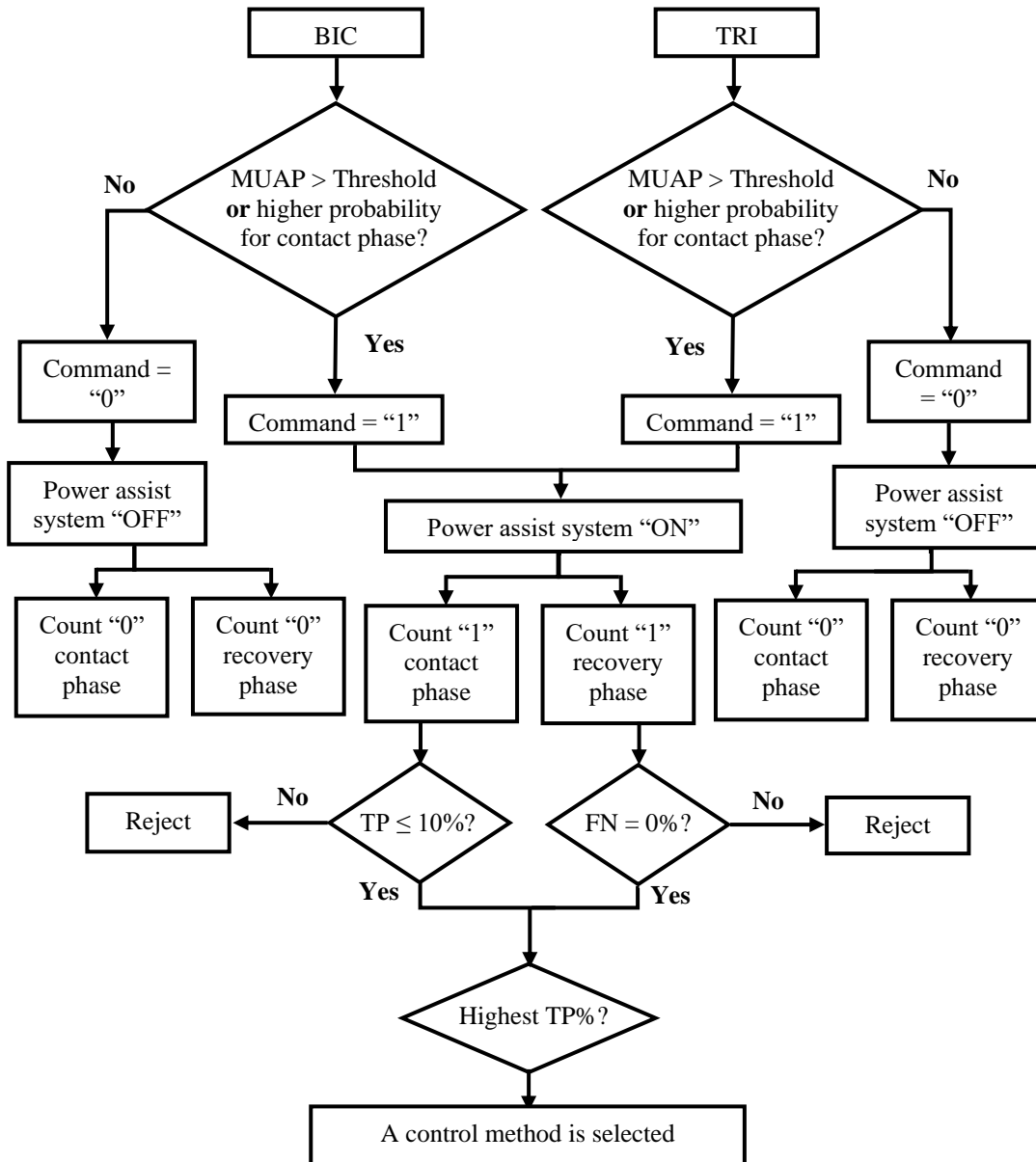


Fig. 7 Algorithm flow in selecting a control method

Table 5. Misclassification matrix scores

Participant	Control Method	TP	TN	FP	FN	Precision (%)	Sensitivity (%)	Specificity (%)	Accuracy (%)
1	PDF	17	937	41	0	29.5	100	95.8	95.9
	MEAN	8	922	50	6	13.9	57.1	94.9	94.9
	SD	4	923	54	1	6.9	80	94.5	94.5
	CI	4	923	54	1	6.9	80	94.5	94.5
	MPD	0	920	58	0	0	-	94.1	94.1
2	PDF	14	930	45	8	23.8	63.6	95.4	95.4
	MEAN	0	924	59	0	0	-	94.0	94.0
	SD	0	924	59	0	0	-	94.0	94.0
	CI	0	924	59	0	0	-	94.0	94.0
	MPD	0	924	59	0	0	-	94.0	94.0
3	PDF	52	976	5	1	91.1	98.1	99.5	99.5
	MEAN	5	930	52	0	8.8	100	94.7	94.7
	SD	0	925	57	0	0	-	94.2	94.2
	CI	0	925	57	0	0	-	94.2	94.2
	MPD	35	960	22	0	61.3	100	97.7	97.7

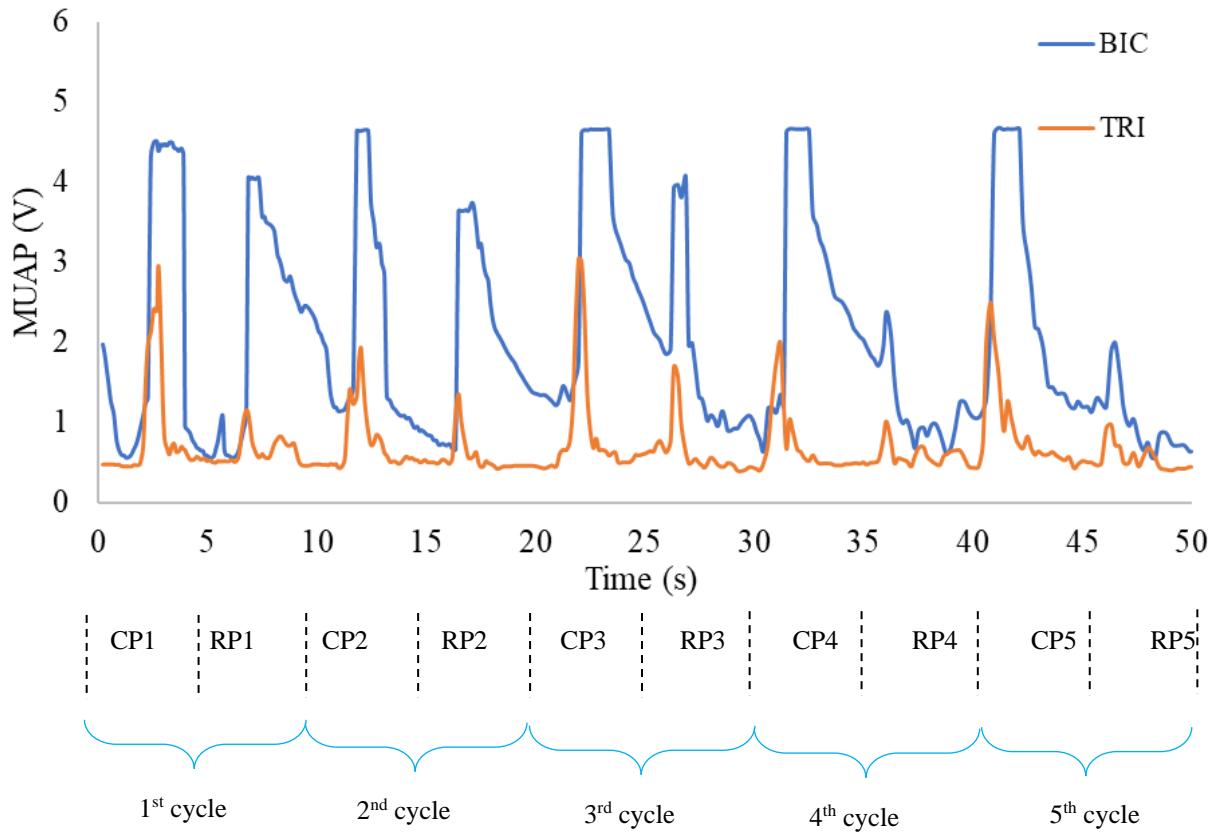


Fig. 8 SEMG signal recorded for one of the participants (CP is contact phase and RP is recovery phase)

Table 6. Classification accuracy for other research

No	Electrode placement	Control method	Classification Accuracy	Device
1 ²⁵	Zygomaticus major and transversus menti (facial muscles)	Pattern-based	64.9%	STM 32F103
2 ²⁶	Flexor (arm muscle)	Pattern-based	98.9%	ATMEGA-8
3 ²⁷	Corrugator and zygomaticus	Pattern-based	93.3%	Myon Aktos
4 ²⁸	Jaw muscles	Pattern-based	85%	Open BCI Cyto n Bio sensing
5 ²⁹	Arms and jaw muscles	Pattern-based	98.5 %	NI USB-6008
6	My study Biceps and Triceps muscles	Pattern and Non-pattern based	95.1%	Arduino Mega 2560

Table 5 shows the misclassification matrix score for TP, TN, FP and FN and the calculated precision, sensitivity, specificity and accuracy percentage. Some control methods have a 0 TP score, showing that the assistive device is powered on (“1”) in all contact phases. Meanwhile, 0 of the FN score means that the assistive device remains off condition (“0”) for every recovery phase.

TN has the highest score because the device must not activate (“0”) for 90% duration of the experiment. Furthermore, FN is where the targeted output is “1”, but the result is “0”.

PDF control method (participant 3) is the most precise control method, 91.1%, because the FP score is low as 5. That means only 5 readings are “0” in class; the targeted output is “1”.

Looking at the sensitivity indicator, there are 3 control methods has a 100% score. Then, both specificity and accuracy indicators have no 100%, and all are above 94%, which is way higher than the acceptable classification accuracy of 90%³⁰.

Based on the result in Table 5, PDF is selected as the best control method for participant 1, no for participant 2 and MPD for participant 3.

Table 6 shows the result of classification accuracy conducted by other researchers. All of them implement pattern-based control methods to recognize the motion of targeted muscles.

It shows that not all patterns are suitable for the participant, as Jang et al. just obtained about 65%³¹. On the other hand, Kundu and the team achieved about 99%³² of classification accuracy. Acceptable classification accuracy for EMG study is above 90%³³.

4. Conclusion

This misclassification matrix applies to selecting the most suitable control method to assist users in propelling a wheelchair. In order to prevent any harm that happens to the user, sensitivity is the most important indicator in deciding which control method is the best. This is because the FN score must be 0, meaning that the assistive device is not powered during the recovery phase.

The recovery phase is when the user’s hand moves back to the A position (Figure 2) and is not propelling forward. Recommendations for a rehabilitation device to consider sensitivity indicators more than others to avoid incidents happening to the users.

Participant 2 had no control method that had 100% of sensitivity, and he had to repeat the experiment until there was a minimum 1 control method that met the requirement. Meanwhile, for participant 3, 2 control methods achieved a sensitivity of 100%.

Then additional indicator is precision to look into how frequently the assistive is powered on during the contact phase. Additional indicators would improve the performance of assistive devices predicting movement desired by users.

Data Availability

The data used to support the findings of this study are available from the corresponding author upon request.

Acknowledgment

The authors would like to thank the Ministry of Higher Education for providing financial support under the Fundamental Research Grant Scheme (FRGS) No. FRGS /1/2019/TK04/UMP/02/15 (University reference RDU1901199) and University Malaysia Pahang for laboratory facilities as well as additional financial support under Internal Research grant RDU210317.

References

- [1] Salzberg, S. L., "On Comparing Classifiers: Pitfalls to Avoid and a Recommended Approach," *Data Mining and Knowledge Discovery*, vol. 1, pp. 317–328, 1997. *Crossref*, <https://doi.org/10.1023/a:1009752403260>
- [2] Peter M. Vitousek et al., "Human Domination of Earth's Ecosystems," *Science*, vol. 1979, no. 277, pp. 494–499, 1997.
- [3] Foody, G. M., "Status of Land Cover Classification Accuracy Assessment," *Remote Sensing of Environment*, vol. 80, no. 1, pp. 185–201, 2002. *Crossref*, [https://doi.org/10.1016/S0034-4257\(01\)00295-4](https://doi.org/10.1016/S0034-4257(01)00295-4)
- [4] W. Kleynhans et al., "Ship Detection in South African Oceans Using a Combination of SAR and Historic LRIT Data," *2013 IEEE International Geoscience and Remote Sensing Symposium-IGARSS*, pp. 1521–1524, 2013. *Crossref*, <https://doi.org/10.1109/IGARSS.2013.6723076>
- [5] Yaodan Xu et al., "Influence of Electrode Configuration on Muscle-Fiber-Conduction-Velocity Estimation Using Surface Electromyography," *IEEE Transactions on Biomedical Engineering*, vol. 69, no. 8, pp. 2414–2422, 2022.
- [6] Wawrzyniak, Z. M et al., "Objective EMG Signal Models Comparison for Gait Diagnostics," *Photonics Applications in Astronomy, Communications, Industry, and High-Energy Physics Experiments*, vol. 11176, pp. 821–829, 2019.
- [7] Narayan Y., "SEMG Signal Classification Using KNN Classifier with FD and TFD Features," *Materials Today Proceedings*, vol. 37, no. 2, pp. 3219–3225, 2021. *Crossref*, <https://doi.org/10.1016/j.matpr.2020.09.089>
- [8] Yogendra Narayan et al., "Elbow Movement Classification of a Robotic Arm Using Wavelet Packet and Cubic SVM," *Communication and Computing Systems*, vol. 605–610, 2017. *Crossref*, <http://dx.doi.org/10.1201/9781315364094-108>
- [9] Kumari, P et al., "Advance Approach Towards Elbow Movement Classification Using Discrete Wavelet Transform and Quadratic Support Vector Machine," *Communication and Computing Systems*, pp. 839–844, 2017. *Crossref*, <http://dx.doi.org/10.1201/9781315364094-151>
- [10] Phinyomark, A., Larracy, R., and Scheme, E., "Fractal Analysis of Human Gait Variability via Stride Interval Time Series," *Front Physiology*, vol. 11, pp. 333, 2020. *Crossref*, <https://doi.org/10.3389/fphys.2020.00333>
- [11] Sidik, M. M, Ghani, S. C, and Padzi, M. M, "Development of a Wireless Surface Electromyography (SEMG) Signal Acquisition Device for Power-Assisted Wheelchair System," *International Journal of Engineering and Advanced Technology*, vol. 8, pp. 3414–3418, 2019. *Crossref*, <https://doi.org/10.35940/ijeat.F9511.088619>
- [12] M. H. Muhammad Sidik et al., "Innovation on Manual Wheelchair for Hemiplegic and Tetraplegic Patients," *International Journal of Engineering and Advanced Technology*, vol. 8, pp. 3419–3425, 2019.
- [13] M. H. Muhammad Sidik, S. A. Che Ghani, and M. N. F. Saniman, "A Real-Time EMG Pattern Recognition Control Method for Activation of Instrumented Wheelchair Power Assist System," *Palarch's Journal of Archaeology of Egypt/Egyptology*, vol. 17, no. 9, pp. 3430–3441, 2020.
- [14] Chikh, S et al., "Arm-Trunk Coordination in Wheelchair Initiation Displacement: A Study of Anticipatory and Compensatory Postural Adjustments during Different Speeds and Directions of Propulsion," *Journal of Electromyography and Kinesiology*, vol. 40, pp. 16–22, 2018. *Crossref*, <https://doi.org/10.1016/j.jelekin.2018.03.001>
- [15] Jingwei Too et al., "Feature Selection Based on Binary Tree Growth Algorithm for the Classification of Myoelectric Signals," *Machines*, vol. 6, no. 4, pp. 65, 2018.
- [16] Bass A et al., "Comparison of the 6-Min Propulsion and Arm Crank Ergometer Tests to Assess Aerobic Fitness in Manual Wheelchair Users with a Spinal Cord Injury," *American Journal of Physical Medicine and Rehabilitation*, vol. 99, pp. 1099–1108, 2020. *Crossref*, <https://doi.org/10.3390/machines6040065>
- [17] Sindall, P. et al., "Practice Improves Court Mobility and Self-Efficacy in Tennis-Specific Wheelchair Propulsion," *Disability and Rehabilitation: Assistive Technology*, vol. 16, no. 4, pp. 398–406, 2021. *Crossref*, <https://doi.org/10.1080/17483107.2020.1761892>
- [18] Riemer J K Vegter et al., "Initial Skill Acquisition of Handrim Wheelchair Propulsion: A New Perspective," *IEEE Transactions on Neural Systems and Rehabilitation Engineering*, vol. 22, pp. 104–113, 2013. *Crossref*, <https://doi.org/10.1109/tnsre.2013.2280301>
- [19] Sapienza, S et al., "On-Line Event-Driven Hand Gesture Recognition Based on Surface Electromyographic Signals," *2018 IEEE International Symposium on Circuits and Systems (ISCAS)*, pp. 1-5, 2018.
- [20] Jingwei Too et al., "Exploring the Relation Between EMG Pattern Recognition and Sampling Rate Using Spectrogram," *Journal of Electrical Engineering and Technology*, vol. 14, pp. 947–953, 2019. *Crossref*, <https://doi.org/10.1007/s42835-019-00083-3>
- [21] Xinyu Jiang et al., "Enhancing IoT Security via Cancelable HD-Semg-Based Biometric Authentication Password, Encoded By Gesture," *IEEE Internet of Things Journal*, vol. 8, no. 22, pp. 16535–16547, 2021. *Crossref*, <https://doi.org/10.1109/JIOT.2021.3074952>
- [22] Too, J et al., "Exploring the Relation Between EMG Pattern Recognition and Sampling Rate Using Spectrogram," *Journal of Electrical Engineering and Technology*, vol. 14, pp. 947–953, 2019. *Crossref*, <https://doi.org/10.1007/s42835-019-00083-3>
- [23] Ruuska, S. et al., "Evaluation of the Confusion Matrix Method in the Validation of an Automated System for Measuring Feeding Behaviour of Cattle," *Behavioural Processes*, vol. 148, pp. 56–62, 2018. *Crossref*, <https://doi.org/10.1016/j.beproc.2018.01.004>

- [24] Arruda, L. M. et al., "Design and Testing of a Textile EMG Sensor for Prosthetic Control," *EAI International Conference on IoT Technologies for Healthcare*, pp. 37–51, 2019.
- [25] Gupta, P et al., "Accelerometer-Based Hand Gesture Controlled Wheelchair," *Imperial Journal of Interdisciplinary Research*, vol. 2, no. 11, 2016.
- [26] Ishii, C., and Konishi, R, "A Control of Electric Wheelchair Using an EMG Based on Degree of Muscular Activity," *2016 Euromicro Conference*, 2016. *Crossref*, <https://doi.org/10.1109/DSD.2016.19>
- [27] Vikram Kehri et al., "A Machine Learning Approach for FEMG Pattern Recognition System to Control Hands-Free Wheelchair," *Proceedings of TRIBOINDIA-2018 an International Conference on Tribology*, 2018. *Crossref*, <https://dx.doi.org/10.2139/ssrn.3347101>
- [28] Marley Xiong et al., "A Low-Cost, Semi-Autonomous Wheelchair Controlled by Motor Imagery and Jaw Muscle Activation," *2019 IEEE International Conference on Systems, Man and Cybernetics (SMC)*, 2019. *Crossref*, <https://doi.org/10.1109/SMC.2019.8914544>
- [29] Rusydi, M. et al., "Robot Mobile Control Based on Three EMG Signals Using an Artificial Neural Network," *Materials Science and Engineering*, vol. 602, no. 1, 2019. *Crossref*, <https://doi.org/10.1088/1757-899X/602/1/012028>
- [30] Rami N.Khushaba et al., "Toward Improved Control of Prosthetic Fingers Using Surface Electromyogram (EMG) Signals," *Expert Systems with Applications*, vol. 39, no. 12, pp. 10731–10738, 2012. *Crossref*, <https://doi.org/10.1016/j.eswa.2012.02.192>
- [31] Giho Jang et al., "EMG-Based Continuous Control Scheme with Simple Classifier for Electric-Powered Wheelchair," *IEEE Transactions on Industrial Electronics*, vol. 63, no. 6, pp. 3695-3705, 2016. *Crossref*, <https://doi.org/10.1109/TIE.2016.2522385>
- [32] Ananda Sankar Kundu et al., "Hand Gesture Recognition-Based Omnidirectional Wheelchair Control Using IMU and EMG Sensors," *Journal of Intelligent and Robotic Systems*, vol. 91, no. (3-4), pp. 529-541, 2018. *Crossref*, <https://doi.org/10.1007/s10846-017-0725-0>
- [33] Anyuan Zhang et al., "Combined Influence of Classifiers, Window Lengths and Number of Channels on EMG Pattern Recognition for Upper Limb Movement Classification," *2018 11th International Congress on Image and Signal Processing, Biomedical Engineering and Informatics (CISP-BMEI)*, 2018. *Crossref*, <https://doi.org/10.1109/CISP-BMEI.2018.8633114>